Chitosan Nano-composite containing Undecatungstosilicate via Cobalt Substitution: Characterization and Evaluation of their Biological Activity

SHIVA ARUN[a], YADVENDRA SINGH[a], AMREEN NAZ[a], PRABHA BHARTIYA[a], KSHAMA SRIVASTAVA[b], SHAHID SUHAIL NARVI[a] AND PRADIP KUMAR DUTTA[a]*

[a] *Department of Chemistry, Motilal Nehru National Institute of Technology, Allahabad-211004, India*

[b] *Department of Pharmaceutical Sciences, Babasaheb Bhimrao Ambedkar University, Lucknow-226025, India*

ABSTRACT

Encapsulation of polyoxometalates into chitosan have drawn tremendous attraction of researchers in biomedical science. Chitosan (CS) is widely studied for its significant biomedical applications. In this study we have synthesized a nano-composite by encapsulating a cobalt substituted lacunary undecatungstosilicate $[CoSiW_{11}O_{39}(H_2O)]^{6-}$, into biocompatible chitosan. The combination of polyoxometalate with chitosan is not merely physical mixture but indeed it is nano-composite formed by electrostatic interaction between anionic polyoxometalate and cationic chitosan. The resulting nano-complex, (CoSLPOM-CS) was characterized by FT-IR, UV-Vis spectra, energy dispersive X-ray (EDX), scanning electron microscopy (SEM), atomic force microscopy (AFM) and Dynamic light scattering (DLS). FTIR and UV-Vis spectra analysis confirms the successful encapsulation of cobalt substituted lacunary polyoxometalate into chitosan. The antibacterial activity of CoSLPOM, chitosan and CoSLPOM-CS were tested against bacterial strains of B. subtilis gram (+) ve and P. aeruginosa gram (-) ve. The CoSLPOM-CS showed enhanced antibacterial activity as compared to bare CoSLPOM and chitosan. The nano-complex, CoSLPOM-CS was further investigated for drug delivery and it exhibited excellent drug loading efficiency.

KEYWORDS: *Chitosan, Nanocomplex, Drug Delivery, Antibacterial assay*

J. Polym. Mater. Vol. **35,** No. 3, 2018, 305-316
© Prints Publications Pvt. Ltd.
Correspondence author e-mail: pkd@mnnit.ac.in
DOI : https://doi.org/10.32381/JPM.2018.35.03.5

1. INTRODUCTION

Chitosan (CS) is obtained by N-deacetylation of chitin which is found lavishly in exoskeleton of shrimps and shells of crustacean. It is the second most abundant polysaccharide found in nature after cellulose [1]. CS is a muco-adhesive and polycationic biopolymer composed of N-acetyl glucosamine and glucosamine linked together by β 1-4 glucosidic bonds as repeating unit. Diverse CS derivatives can be produced by modifying the free amine and hydroxyl groups of CS [2]. It also offers a high degree of biocompatibility and activity including antifungal, insecticidal and wound healing properties [3]. CS has been widely explored as a carrier for the delivery of various genes, drugs and vaccines. Hence, the combination of different drugs types with CS or its derivatives provides multiple therapeutic advantages, like passive drug targeting, prolonged drug circulation time and reduction of side effects [4]. In human body, biocompatible CS is degraded by chitosanase and lysozyme enzymes, which thus stimulate the release of drug in precise and controlled manner [5].

Polyoxometalates (POMs) are a prominent class of stable transition metal (mostly W, Mo, V) oxo-clusters in their high oxidation states with diversity in composition and size, hence they have attracted attention for their applications in diverse spectrum of magnetic, catalytic, luminescent, biomedical, dye degradation and other properties [6]. Since, POMs are proved important tools for application in antibacterial, antiviral and anticancer activities, there are increasing number of research on polyoxometalate (POM)-based systems [7]. Furthermore, hetero-substituted POMs, incorporating redox-active transition metals, such as Mn, Fe, Co or Ru, have been reported to mimic the activity of natural oxygenase enzymes, by promoting multi-electron processes in aqueous media [8]. New inorganic drugs of low cost, easily tunable and broadly applicable against an entire spectrum of diseases may be developed by these ideal prototype POMs [9]. Encapsulation or conjugation of bioactive POMs into biodegradable polymers like CS, provide new avenues for development of drugs [10-15] having high potential bioactivity [16] with reduced toxicity, effective bio-distribution and greater stability at different pH [17].

In the present research work we have synthesized Keggin structural lacunary polyoxometalate $K_8[SiW_{11}O_{39}].13H_2O$ (LPOM) from its parent saturated compound ($K_8[SiW_{12}O_{40}].xH_2O$) by removing one tungstate unit from SiW_{12} molecule [18]. The LPOM shows better antibacterial activity as compared to its parent compound [19]. The lacuna of LPOM was blocked by substituting metal cation (Co^{2+}) to form a compound known as "lacunary substituted" (hetero) polyoxotungstate ($K_6[SiW_{11}O_{39}Co(H_2O)].14H_2O$) [hereafter abbreviated as CoSLPOM] [18]. The cobalt substituted lacunary POM species (CoSLPOM) thus synthesized, was encapsulated into CS forming a nano-complex. Antibacterial activity of CoSLPOM, chitosan and their nano-complex were tested against two bacterial strains of *B. subtilis gram (+) ve and P. aeruginosa gram (-) ve*. and the material was further studied for drug delivery.

2. EXPERIMENTAL

2.1 Materials and Characterization Techniques

CS (low molecular weight), silicotungstic acid $H_4[SiW_{12}O_{40}].xH_2O$ and $Co(NO_3).6H_2O$ were purchased from Sigma Aldrich. Acetic acid, potassium bicarbonate, ethanol were purchased from CDH and are of A.R. grade. Nutrient agar and Nutrient broth were purchased from Titan Biotech Ltd. Rajasthan, India. The test strain *B. subtilis*, *gram (+) ve.* bacteria and *P. aeruginosa gram (-) ve*. bacteria were obtained from IMTECH, Chandigarh, India. FT-IR spectra were recorded in the range of wave number 4000–400 cm^{-1} using KBr disks with Perkin Elmer spectrophotometer. Nova Nano FE-SEM 450 (FEI) is coupled to EDX detector for measuring the elemental composition of material. Topographical characteristics of nano-composite was studied with AFM (Agilent technologies). UV–visible spectra were obtained with Shimadzu UV-2450. Particle size measurement was accomplished by DLS technique using Nano Microtrac total solution in the particle characterization software. ICP-AES analysis was performed by SPECTRO Analytical Instruments GmbH-ARCOS, Simultaneous ICP Spectrometer.

2.2.1. Preparation of cobalt substituted lacunary POM species (CoSLPOM)

The cobalt substituted lacunary POM (CoSLPOM) was synthesized according to the procedure as reported by Tajima et al [18] and the molecular formula of CoSLPOM ($K_6[SiW_{11}O_{39}Co(H_2O)].14H_2O$) was confirmed by inductively coupled plasma atomic emission spectroscopy (ICP-AES). The calculated and found percent by ICP-AES data for CoSLPOM having chemical formula ($K_6[SiW_{11}O_{39}Co(H_2O)].14H_2O$); Calculated% Co,1.85; K,7.25; Si,0.87; W,62.43; found% Co, 1.84; K,7.28; Si,0.89; W,62.46.

2.2.2. Preparation of CoSLPOM-Chitosan nano-complex (CoSLPOM-CS)

In order to synthesize nano-complex comprising of CS and cobalt substituted lacunary POM, chitosan was dissolved in 2% v/v acetic acid to give concentrations of 0.50% w/v. The CS solution was filtered to remove any suspended particles and heated at 50°C for 2 hours with continuous stirring and then cooled to room temperature (Solution1). pH of above solution (Solution 1) was maintained at 5.0 with NaOH. 0.1 gm of CoSLPOM was dissolved in minimum amount of milli-Q water (Solution 2). Solution 2 was added to Solution 1 drop-wise under the controlled sonication for 10 minutes resulting into a stable colloidal suspension of CoSLPOM and CS nano-complex which is hereafter abbreviated as CoSLPOM-CS. This colloidal suspension containing nano-complex of CoSLPOM-CS was stirred at room temperature for 10 hours (h) and then centrifuged for 20 minutes (min), at 20,000rpm to collect CoSLPOM-CS. The nano-complex of CoSLPOM-CS was collected and washed with milli-Q water several times and dried under vacuum.

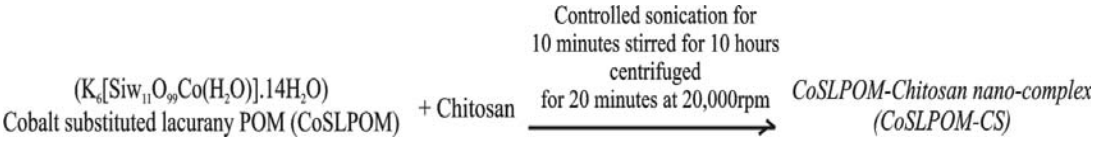

Scheme 1. Preparation of CoSLPOM-Chitosan nano-complex (CoSLPOM-CS)

3. Evaluation of hybrid material

3.1. Antibacterial assessment

The antimicrobial activity of cobalt substituted LPOM $[CoSiW_{11}O_{39}(H_2O)]^{6-}$, chitosan and their nanocomposite CoSLPOM-CS were tested against two bacterial strains of *B. subtilis gram (+) ve and P. aeruginosa gram (-) ve*. Antimicrobial test was performed by using agar disc diffusion method [20]. In brief, nutrient agar media (28 g/L in water) and nutrient broth (13 g/L in water) were prepared. The nutrient agar media was then poured into autoclaved petri dishes. The active broth culture of each bacterial strain was spread on nutrient agar plates. In inoculated agar plates were treated with

50 µg of CoSLPOM, chitosan and CoSLPOM-CS nanocomposite in 100 µl of aqueous solution and put in wells (10 mm) with control (water). The incubation was continued for 14 h at 37°C, when finally the zone of inhibition around disc was measured in (mm) to determine the antibacterial efficacy.

3.2. Curcumin loaded CoSLPOM-CS nano-composite (CoSLPOM-CS-Cur)

CS and CoSLPOM solution were prepared as described above. Curcumin was dissolved in ethanol to give a final concentration of 1mg/mL. Curcumin solution was added drop-wise into the CS solution under the controlled sonication, followed by addition of CoSLPOM solution and sonication was further continued for 1 h. The suspension which is obtained after sonication was stirred for 12 h and then centrifuged for 25 min, at 20,000rpm. After centrifugation the curcumin loaded nanocomplex (CoSLPOM-CS-Cur) was washed several times with ethanol in order to remove non encapsulated curcumin. The supernatant was collected and stored to calculate encapsulation and loading efficiency. The obtained material was lyophilized and stored at 4°C for further use.

3.3. Encapsulation Efficiency (EE) and Drug Loading Efficiency (LE) of CoSLPOM-CS-Cur

The EE and LE CoSLPOM-CS-Cur nano-complex were determined by measuring the concentration of free drug in the dispersion medium by centrifugation at 10,000rpm for 20 minutes. The supernatant obtained was diluted with 90% ethanol, and the drug concentration in the resultant solution was measured at 420 nm by UV-VIS with a standard curve. Following formulas were used to calculate the EE and LE.

$$EE = \frac{\text{Total curcumin} - \text{Free curcumin}}{\text{Total Curcumin}} X\ 100\%$$

$$LE = \frac{\text{Total Curcumin} - \text{Free curcumin}}{\text{Weight of freeze} - \text{dried nanoparticles}}\ X\ 100\%$$

where the free Curcumin is the analyzed weight of drug in supernatant, total Curcumin is the feeding weight of drug in the preparation of NPs, and the weight of freeze-dried NPs is the total weight of carrier.

3.4 In vitro release study

In vitro curcumin release profiles from CoSLPOM-CS-Curcumin were determined as follows:

Lyophilized CoSLPOM-CS-Curcumin obtained so were re-dispersed in 22 mL of 0.01 M phosphate-buffered saline solution (pH 7.4 and pH 5.0) at a final concentration of 150 µg/mL. Total volume was divided into 11 Eppendorf tubes giving 11 different sets for time-dependent release study at time intervals of 0, 2, 4, 6, 12, 24, 36, 48, 60, 72 and 96 h. All sets were incubated at 37°C under gentle agitation. At proper time intervals, intake (or release) amounts of curcumin in loaded NPs were first extracted in methanol and quantified spectrophotometrically. The release was quantified as follows:

$$\text{Release (\%)} = \frac{\text{Released curcumin}}{\text{Total Curcumin}}\ X\ 100\ \%$$

4. RESULT AND DISCUSSION

4.1.1. FT-IR spectra

FT-IR (cm^{-1}) spectrum of CS in Fig. 1(a) and CoSLPOM in Fig. 1(b) exhibit similar peaks as reported in literature. CS shows characteristic peak at 1636 corresponding to N-H bending vibration (amines) and the peak at 1072 is due to the bridge oxygen (C-O-C) stretching vibration [21]. In CoSLPOM the peaks at 460 and 424 were due to stretching vibration of Co-O bond [22], 535 (υ_{sym}W-O-W), 725 (υ_{asym}W-O-W), 797 ((υ_{asym}W-O-W), 868 (υ_{asym}W-O-W), 890 (υ_{asym}W-O-W), 962 (υ_{asym}W=O) [23]. FT-IR spectrum of CoSLPOM-CS nano-composite (Fig. 1c) exhibit broad peak ~ 3400 corresponding to –OH group and the peak at 1630 is due to N-H bend of $–NH_2$. Further, the presence of characteristic FT-IR peaks that were present in chitosan and CoSLPOM in CoSLPOM-CS with minor shifts indicate the encapsulation of CoSLPOM into chitosan.

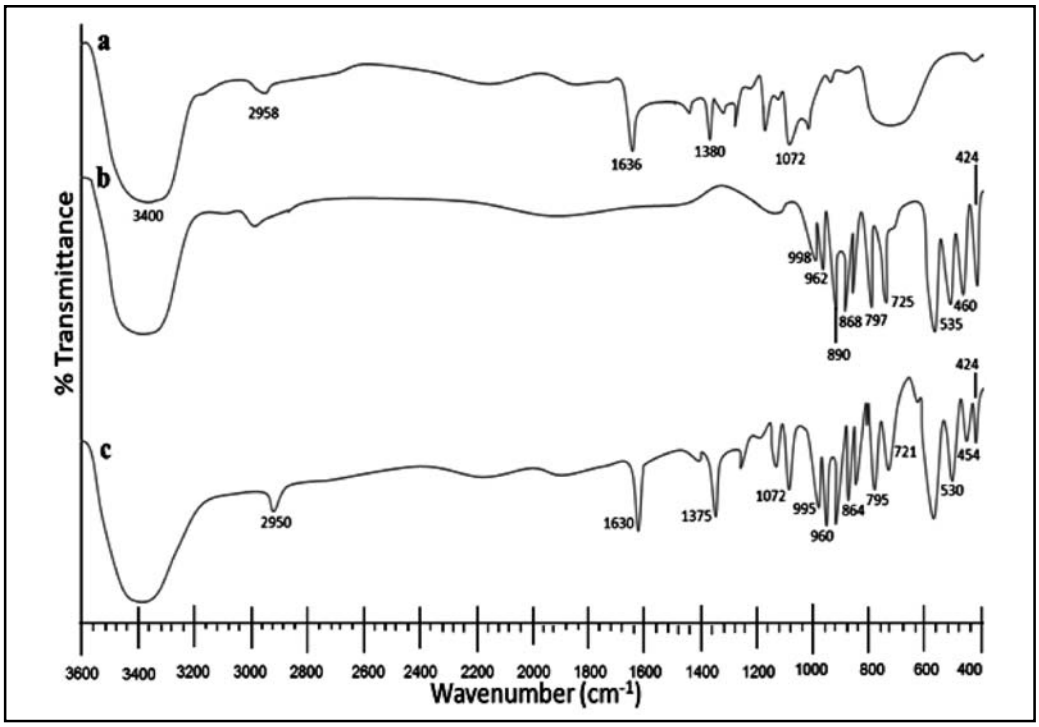

Fig. 1. FT-IR (cm^{-1}) spectra (a) CS (b) CoSLPOM (c) CoSLPOM-CS

4.1.2. EDX and ICP Analysis

EDX analysis of nano-composite shows the presence of all expected elements i.e. C, N, O and it also reveals that the stoichiometric ratio of Co to W atom in CoSLPOM-CS nano-complex is 1 Co atom per 11 W atoms (Fig. 2). The result of EDX analysis was further corroborated by ICP technique. ICP exhibited the presence of W, Si and Co in the same amount as expected in the nano-composite, found% Co,0.62; K,2.29; Si,0.25; W,20.80.

4.1.3. SEM and AFM Image

SEM image (Fig. 3a) of CoSLPOM-CS shows monodispersed nanoparticles with spherical morphology. The AFM image (Fig. 3b) display smooth, uniform and spherical structure of CoSLPOM-CS which endorse that CoSLPOM is incorporated into CS.

4.1.4. DLS analysis

DLS analysis (Fig. 4a) shows that around 85% particles possess size below 100nm making them a good candidate for drug delivery vehicles. The DLS histogram reveals that synthesized particles have excellent size distribution between 60 to 130 nanometer, about 39% particles having size about 71 nm. No considerable change was observed after encapsulation of curcumin in CoSLPOM-CS as observed by Fig. 4(b).

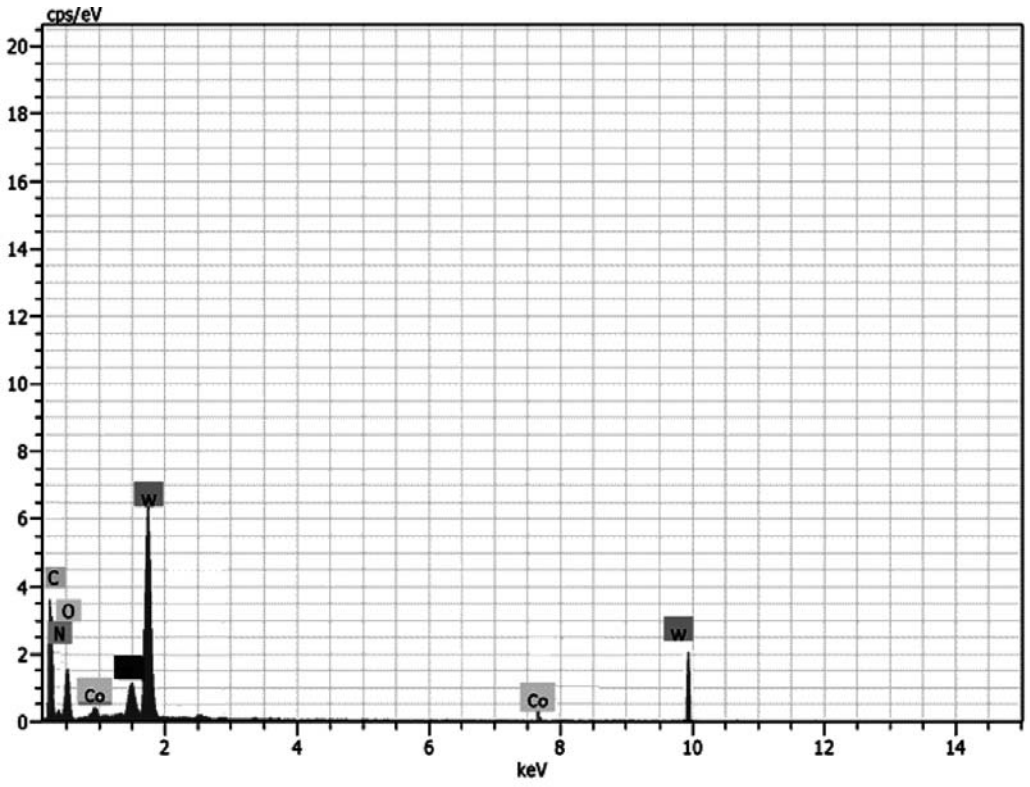

Spectrum: Acquisition 226

El	AN	Series	C norm. [wt.%]	C Atom. [at.%]
C	6	K-series	31.42	44.20
O	8	K-series	20.20	29.21
Si	14	K-series	1.89	0.85
N	7	K-series	9.20	5.10
W	74	L-series	34.18	18.92
Co	29	K-series	3.11	1.72
		Total:	100.00	100.00

Fig. 2. EDX of CoSLPOM-CS

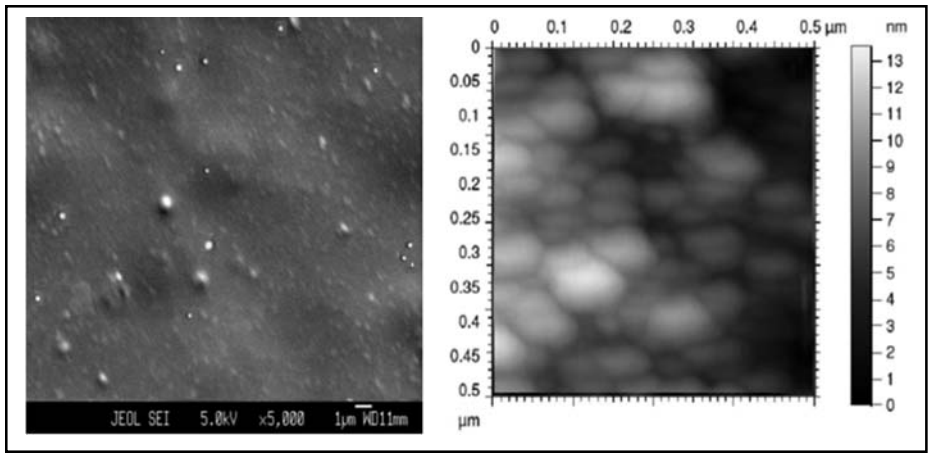

Fig. 3. (a) SEM image of CoSLPOM-CS (b) AFM image of CoSLPOM-CS

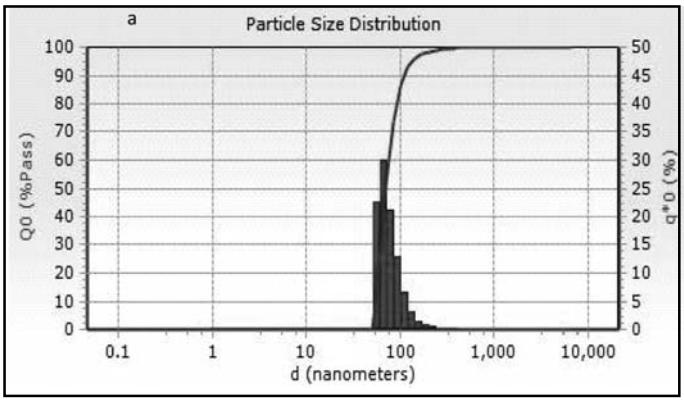

Fig. 4. (a) DLS analysis of CoSLPOM-CS

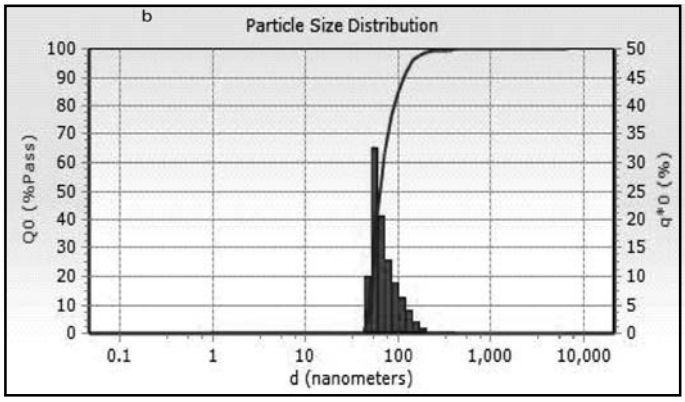

Fig. 4. (b) DLS analysis of CoSLPOM-CS-Curcumin

4.1.5. UV-Vis Spectroscopy

The encapsulation of CoSLPOM into chitosan was further investigated through UV-Vis spectroscopy (Fig. 5). Firstly, UV-Vis spectra of CoSLPOM of known concentration was recorded which shows absorption around 265 nm. Four readings of UV-Vis spectra was taken during CoSLPOM-CS synthesis keeping the same concentration of CoSLPOM. First reading of supernatant was taken just after sonication was stopped, second reading of supernatant was taken after two hours of continuous stirring of colloidal suspension of CoSLPOM-CS. Third reading was taken after ten hours of continuous stirring and fourth reading of supernatant was taken after centrifugation. The first reading shows the presence of typical absorption peak of CoSLPOM around 265 nm and in second reading this peak got diminished which shows that CoSLPOM is entrapped into CS. The characteristic peak around 265 nm finally vanished in the third and fourth reading of UV-Vis spectra. This clearly indicate that CoSLPOM was successfully encapsulated into CS after centrifugation.

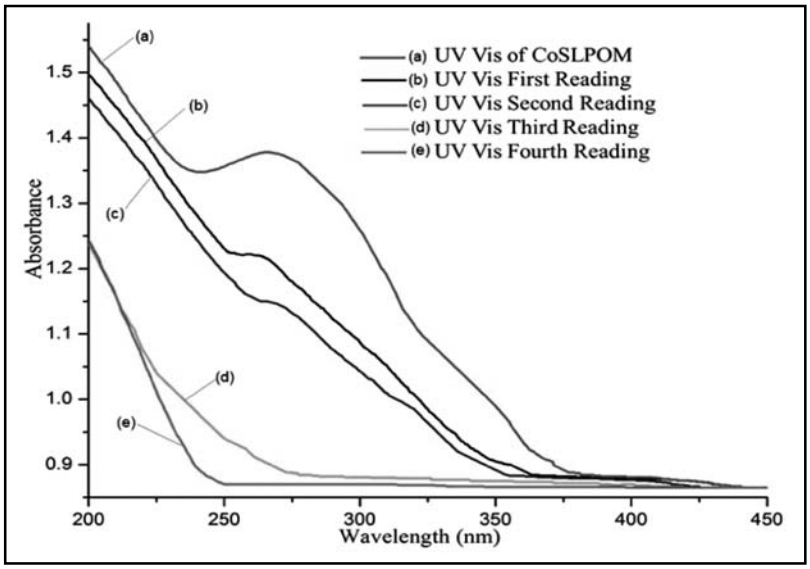

Fig. 5. UV Vis Spectra of (a) CoSLPOM (b) First Reading was taken just after sonication of CoSLPOM-CS was stopped (c) Second reading after two hours of continuous stirring of colloidal suspension of CoSLPOM-CS (d) Third Reading after ten hours of continuous stirring of colloidal suspension of CoSLPOM-CS (e) Fourth Reading was taken after centrifugation of CoSLPOM-CS

4.1.6. Antibacterial assessment

The antibacterial properties of CoSLPOM, CS and their nanocomplex CoSLPOM-CS have been tested against two bacterial strains *B. subtilis* (gram + ve) and *P. aeruginosa* (gram – ve), the effect of nano-composite and individual component (inhibitory zone) data are tabulated in (Table 1). CoSLPOM have shown significant growth inhibitory effects on gram (+) ve but

less significant on gram (-) ve bacteria. The inhibitory effects of CoSLPOM-CS against *B. subtilis* and *P. aeruginosa* bacteria are shown in (Fig. 6). Chitosan itself has antibacterial activity and most acceptable antimicrobial mechanism of chitosan is due to the presence of charged groups, which form by protonation of amino groups [NH_2^+] in their polymer chain and which form ionic interactions with bacteria wall constituents. This interface may be leading to the hydrolysis of the peptidoglycans membrane in the microorganism wall, provoking the leakage of intracellular electrolytes, leading the bacterial to death. The data represent that CoSLPOM-CS do show potential antimicrobial activity against both gram positive and negative. It is clear from the figure CoSLPOM not shown itself major antibacterial activity, whereas chitosan itself have potential antimicrobial activity. But when CoSLPOM is formed nano-complexed with chitosan, then chitosan bio-activity got synergistically increased (Table 1). CoSLPOM has not shown major growth inhibitory effect against gram (-) ve bacteria.

TABLE 1. The measured values of inhibitory zone (mm) by antibacterial activities of CoSLPOM, chitosan and nanocomplex against B. subtilis (gram + ve) & P. aeruginosa (gram - ve) bacteria

	Diameters of inhibitory zone (mm)	
Samples	*B. subtilis*(gram + ve)	*P. aeruginosa*(gram –ve)
$[CoSiW_{11}O_{39}(H_2O)]^{6-}$	5.2 ± 0.2	Nd*
Chitosan	23.7 ± 0.3	22.6 ± 0.4
CoSLPOM-CS Nano-complex	34.5 ± 0.9	27 ± 0.7

*Not determinable

A possible explanation of this observation lies in the difference in composition of outer membrane of gram (+) ve and gram (-) ve bacteria. Gram (+) ve bacterial cell walls are rich in lipoproteins and phospholipids than gram (-) ve bacteria which might enhance the permeability of cobalt related compounds which

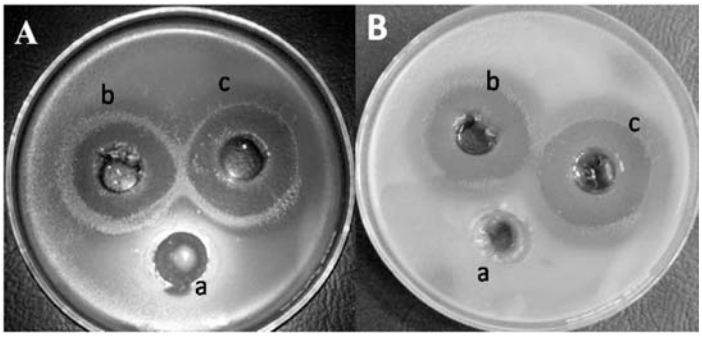

Fig. 6. Images of antibacterial effect (inhibitory zone) of $[CoSiW_{11}O_{39}(H_2O)]^{6-}$ (a) chitosan (b)and their CoSLPOM-CS nanocomposite (c) against gram (+) ve bacteria *B. subtilis* (121, A) & gram (-) bacteria *P. aeruginosa* (1688, B)

is present in polyoxometalate complex [24]. Another argument in favor of above observation relates to the inherent defense mechanism adopted by the gram (-) ve bacteria owing to the presence of unique periplasmic space which is not present in gram (+) ve bacteria. The opposition of gram negative bacteria towards antibacterial agents lies in the presence of hydrophilic surface of their outer membrane which is rich in lipoproteins and lipopolysaccharide causing a barrier to the diffusion of antimicrobial agent [25].

We conclude that the enhanced antimicrobial properties, shown by the CoSLPOM-CS nanocomplex is largely due to hydrophobicity, lipophilicity and capability of this compound to bind with proteins at acidic pH [26].

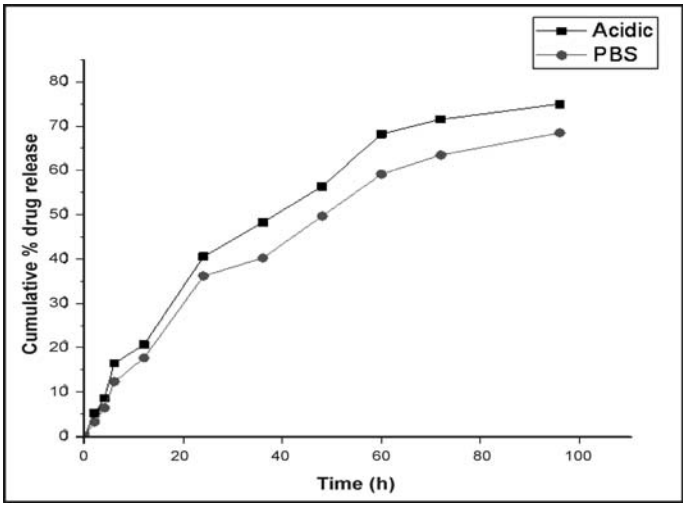

Fig. 7. Drug Release Profile of CoSLPOM-CS-Curcumin in neutral and acidic medium

4.1.7. Entrapment Efficiency, drug loading and in vitro drug release studies

Entrapment efficiency and loading efficiency of Curcumin loaded CoSLPOM-CS nano-complex (CoSLPOM-CS-Curcumin) was found to be 71% and 4.1%.

Fig. 7 shows that drug release study of prepared CoSLPOM-CS-Curcumin in neutral and in acidic medium. In neutral medium, only 68.46% of the drug release was observed whereas in acidic medium it is 74.96%. The analysis shows faster drug release in acidic medium as compared to neutral pH.

5. CONCLUSION

A nanocomplex was synthesized by encapsulating cobalt substituted lacunary polyoxometalate (CoSLPOM) into CS. The formation of CoSLPOM-CS was confirmed by relevant characterization techniques. Antimicrobial activity of CoSLPOM, chitosan and their nano-composite CoSLPOM-CS were tested against two bacterial strains *of B. subtilis gram (+) ve and P. aeruginosa gram (-) ve*. The nanocomplex showed enhanced antibacterial activity as compared to chitosan and CoSLPOM. The prepared

CoSLPOM-CS exhibit excellent drug encapsulation and loading efficiency. Drug release profile of synthesized nanocomplex shows a pH-modulated drug release 68.46% (at pH 7.4) while a higher 74.96% drug release was observed at pH 5.0. CS encapsulated nanocomplex, CoSLPOM-CS may have significant application in biomedical researches.

Acknowledgment

The authors are grateful to Centre for interdisciplinary research (CIR) facility, MNNIT, Allahabad, Malaviya National Institute of Technology, Jaipur for performing FTIR analysis and SAIF, IIT Bombay for EDX measurements. Prof. S. S. Narvi is also thankful to the funding agency Council of Science and Technology, Lucknow.

REFERENCES

1. P. K. Dutta, J. Dutta, M. C. Chattopadhyaya, V. S. Tripathi, *J. Polym. Mater*., 21 (2004) 321-333.
2. (a) A. Anitha, V. V. Divya Rani, R. Krishna, V. Sreeja, N. Selvamurugan, S. V. Nair, *Carbohydrate Polymers*, 78 (2009) 672–677; (b) R. Jayakumar, N. Nwe, S. Tokura, H. Tamura, *International Journal of Biological Macromolecules*, 40 (2007) 175–181; (c) R. Jayakumar, M. Prabaharan, S. V. Nair, S. Tokura, H. Tamura, N. Selvamurugan, *Progress in Materials Science*, 55 (2010) 675–709. (d) R. Jayakumar, M. Prabaharan, R. L. Reis, J. F. Mano, *Carbohydrate Polymers*, 62 (2005) 142–158.
3. (a) D. Archana, J. Dutta, P. K. Dutta, *International Journal of Biological Macromolecules*, 57 (2013) 193-203. (b) D. Archana, B. K. Singh, J. Dutta, P. K. Dutta, *International Journal of Biological Macromolecules*, 73 (2015) 49-57. (c) B. K. Singh, R. Sirohi, D. Archana, A. Jain P. K. Dutta, *International Journal of Polymeric Materials and Polymeric Biometarials*, 64 (2014) 242-252. (d) Z. Guo, R. Chen, R. Xing, S. Liu, H. Yu, P. Wang, C. Li, P. Li, *Carbohydr. Res.,* 341 (2006) 351–354; (e) E. I. Rabea, M. El Badawy, T. M. Rogge, C. V. Stevens, M. Hçfte, W. Steurbaut, G. Smagghe, *Pest Manage. Sci*., 61 (2005) 951–960; (f) M. Abe, M. Takahashi, S. Tokura, H. Tamura, A. Nagano, *Tissue Eng.,* 10 (2004) 585 –594.
4. P. K. Dutta, J. Dutta, V. S. Tripathi, *J. Sci. Ind. Res*., 63 (2004) 20–31.
5. (a) S. F. Peng, M. T. Tseng, Y. C. Ho, M. C. Wei, Z. X. Liao, H. W. Sung, *Biomaterials* 32 (2011) 239–248. (b) Q. Zhao, X. Feng, S. Mei, Z. Jin, *Nanotechnology* 20 (2009) 105101.
6. D. L. Long, E. Burkholder, L. Cronin, *Chem. Soc. Rev*., 36 (2007) 105 – 121; (b) T. Yamase, M. T. Pope, Polyoxometalate Chemistry for Nano-Composite Design, Kluwer, Dordrecht, 2002; (c) H.U.V. Gerth, A. Rompel, B. Krebs, J. Boos, C. Lanvers-Kaminsky, *Anti-Cancer Drugs*, 16 (2005) 101 –106.
7. (a) B. Hasenknopf, *Front. Biosci*., 10 (2005) 275 – 287; (b) J. T. Rhule, C. L. Hill, D. A. Judd, R. F. Schinazi, *Chem. Rev.,* 98 (1998) 327 – 357; (c) D. A. Judd, J. H. Nettles, N. Nevins, J. P. Snyder, D. C. Liotta, J. Tang, J. Ermolieff, R. F. Schinazi, C. L. Hill, *J. Am. Chem. Soc.,* 123 (2001) 886–897; (d) M. Witvrouw, H. Weigold, C. Pannecouque, D. Schols, E. De Clercq, G. Holan, *J. Med. Chem*., 43 (2000) 778 –783; (e) S. Shigeta, S. Mori, T. Yamase, N. Yamamoto, *Biomed. Pharmacother*., 60 (2006) 211 –219.
8. (a) A. Sartorel, M. Carraro, G. Scorrano, B. S. Bassil, M. H. Dickman, B. Keita, L. Nadjo, U. Kortz, M. Bonchio, *Chem. Eur. J*., 15 (2009) 7854 – 7858; (b) A. Sartorel, M. Carraro, R. De Zorzi, S. Geremia, N. D. McDaniel, S. Bernhard, G. Scorrano, M. Bonchio, *J. Am. Chem. Soc.,* 130 (2008) 5006 –5007; (c) M. Bonchio, M. Carraro, A. Sartorel, G. Scorrano, U. Kortz, *J. Mol. Catal. A: Chem*., 251 (2006) 93– 99.
9. G. Geisberger, S. Paulus, M. Carraro, M. Bonchio, G. R. Patzke, *Chem. Eur. J*., 17 (2011) 4619 – 4625.

10. L. Zhang, J. M. Chan, F. X. Gu, J.-W. Rhee, A. Z. Wang, A. F. Radovic-Moreno, F. Alexis, R. Langer and O. C. Farokhzad, *ACS nano*, 2 (2008) 1696-1702.

11. K. A. Whitehead, R. Langer and D. G. Anderson, *Nature reviews Drug discovery*, 8 (2009) 129-138.

12. N. Bertrand and J.-C. Leroux, *J. Controlled Release*, 161 (2012) 152-163.

13. V. M. Pandya, U. Kortz and S. A. Joshi, *Dalton Trans*., 44 (2015) 58-61.

14. H. S. Shah, R. Al-Oweini, A. Haider, U. Kortz and J. Iqbal, *Toxicol. Rep*., 1 (2014) 341-352.

15. J. Zhou, P. Yin, X. Chen, L. Hu, T. Liu, *Chem.Comm*., 51 (2015) 15982-15985.

16. (a) M. Bonchio, M. Carraro, G. Scorrano, E. Fontananova, E. Drioli, *Adv. Synth. Catal.,* 345 (2003) 1119 – 1126. (b) G. Geisberger, S. Paulus, M. Carraro, M. Bonchio, G.R. Patzke, *Chem. Eur. J*. 17 (2011) 4619–4625. (c) T. Meißner, R. Bergmann, J. Oswald, K. Rode, H. Stephan, W. Richter, H. Zänker, W. Kraus, F. Emmerling, G. Reck, *Transit. Met. Chem*. 31 (2006) 603–610. (d) Y. Feng, Z. Han, J. Peng, J. Lu, B. Xue, L. Li, H. Ma, E. Wang, *Mater. Lett*. 60 (2006) 1588–1593. (e) D. Menon, R.T. Thomas, S. Narayanan, S. Maya, R. Jayakumar, F. Hussain,V.K. Lakshmanan, S. Nair, *Carbohydr. Polym*. 84 (2011) 887–893. (f) G. Geisberger, E.B. Gyenge, C. Maake, G.R. Patzke, *Carbohydr. Polym*. 91 (2012) 58–67.

17. F. Zhai, D. Li, C. Zhang, X. Wang, R. Li, *European Journal of Medicinal Chemistry* 43 (2008) 1911-1917.

18. Y. Tajima, *Biol. Pharm. Bull*., 24 (2001) 1079—1084.

19. B. Hasenknopf, *Frontiers in Bioscience*, 10 (2005) 275—287.

20. S. Tripathi, G. K. Mehrotra, P. K. Dutta, *Bull. Mater. Sci*., 34 (2011) 29–35.

21. D. Menon, R. T. Thomas, S. Narayanan, S. Maya, R. Jayakumar, F. Hussain, V. K. Lakshmanan, S. V. Nair, *Carbohydrate Polymers*, 84 (2011) 887–893.

22. K. Kamoto, P. J. Mccarthy, A. E. Martell, Infrared Spectra of Metal Chelate Compounds. III. Infrared Spectra of Acetylacetonates of Divalent Metals, Contribution from Jeppson Laboratory of Chemistry, Clark University, Worcester, Massachusetts, 83 (1960) 1272-1276.

23. Z. Xin, J. Peng, T. Wang, B. Xue, Y. Kong, L. Li, E. Wang, Keggin POM *Inorganic Chemistry*, 45 (2006) 8856-8858.

24. G. Fiorani, O. Saoncella, P. Kaner, S. A. Altinkaya, A. Figoli, M. Bonchio, M. Carraro, *J. Clust. Sci*., 25 (2014) 839-854.

25. C. Gao, S. Mao, C.-H. L. Lo, P. Wirsching, R. A. Lerner, K. D. Janda, *Proc Natl Acad Sci* U S A 96 (1999) 6025–6030.

26. S. Aguado, J. Quirós, J. Canivet, D. Farrusseng, K. Boltes, R. Rosal, *Chemosphere,* 113 (2014) 188-192.

Received: 25-09-2018

Accepted: 26-10-2018